Haptic Display With an Interface Device Capable of Continuous-Time Impedance Display Within a Sampling Period

Masayuki Kawai and Tsuneo Yoshikawa, *Fellow, IEEE*

Abstract—**Stability of a haptic interface is an important issue in virtual reality because an operator directly touches haptic interface devices. Stability is influenced by the sampling period and the discrete-time property of the control system. For decreasing the sampling system influence, this paper proposes a haptic device with an analog circuit which is placed between the computer and the haptic device. The circuit functions as springs and dampers. The control system can specify stiffness, damping coefficients, and their equilibrium. Since the impedance generated by the electric spring and damper can work continuously within the sampling period, it is effective for making the system more stable. We also develop a control method for displaying a static virtual object with the proposed device. Further, we discuss the effects of the proposed approach analytically, using passivity analysis for a 1-degree-of-freedom display system. Finally, some experimental results in a two-dimensional virtual environment are presented.**

Index Terms—**Electric circuit, haptic interface, impedance control, passivity analysis, stability, virtual reality.**

I. Introduction

HAPTIC interfaces are useful devices for operators to touch and feel virtual environments composed by computers. In this technology, because an operator has to make direct contact with display devices and unstable behavior might damage the operator, haptic interface stability is a crucial problem.

In many haptic interfaces, coupling impedance or simple stiffness is used between a haptic device and virtual objects [1], [6], [12]. A number of researchers have studied stability issues in haptic interaction and coupling impedance tuning. Minsky *et al.* [2] discussed a tradeoff relation among simulation rates, virtual wall stiffness and viscosity of haptic display devices for simple virtual environments. Colgate and Schenkel [3], Colgate *et al.* [4], and Colgate and Brown [8] discussed passivity of a haptic display for a simple virtual wall and a moving object using a tool-type device. They derived conditions under which the haptic display would exhibit passive behavior. Such fundamental stability and performance issues are well discussed by Adams and Hannaford [5] with a two-port model, which is a common method of analyzing stability and performance in bilateral tele-operation. In these studies, the root of problems is that the system includes a sampling operation. When the sampling period is longer, it becomes more difficult to keep the system stable and coupling impedance should be set low. It means that the operator feels that the surface is soft and that it is not suitable for displaying a hard surface with long sampling periods. To avoid long sampling periods in a simulation with complex virtual environments, some systems have been proposed using distributed systems in which a global environment is calculated in long sampling periods; a local environment near an operator is simulated in a local system with small sampling periods [9]–[11]. However, it is inevitable that the local system perfectly avoids discrete-time property.

This paper proposes a new haptic device with an electric spring and damper on each joint; it decreases the influence of discrete-time property on the stability and expands a range of stable coupling impedance. The control system can specify stiffness, damping coefficients and their equilibriums. Since impedance generated by the electric spring and damper can work continuously within the sampling period, this approach is effective for decreasing sampled-data system influence. First, we present the basic concept of this device and a method for displaying a static virtual object which rests still in the virtual environment. Then, we discuss the effect of the approach using passivity analysis for a 1-degree-of-freedom (DOF) display system. Finally, experiments for the case of a two-dimensional (2-D) virtual environment are performed.

II. Haptic Interface With Continuous-Time Impedance

A. Conventional Haptic Device

A number of conventional haptic interfaces use devices that exert reference force specified by a computer through a digital–analog converter (DAC) (see Fig. 1). Since the computer is a sampled-data system, force is exerted discretely. For decreasing unstable behavior caused by the discrete-time property in such a system, coupling impedance is virtually set between the haptic devices and the virtual environment. Coupling impedance must be calculated in a discrete-time system along with dynamic simulation of the virtual object and virtual environment. Therefore, stability is influenced by the sampling period even if the virtual object is static.

B. Haptic Device With Electric Circuit Generating Continuous-Time Impedance

This paper proposes a haptic interface with an analog circuit generating impedance for decreasing the sampling period influence. Fig. 2 shows the device in the case of a 2-DOF system.

Manuscript received March 13, 2002; revised June 2, 2003.

M. Kawai is with the Center for Cooperative Research in Science and Technology, Fukui University, Fukui 910-8507, Japan (e-mail: mkawai@mech.fukui-u.ac.jp).

T. Yoshikawa with the Department of Mechanical Engineering, Kyoto University, Kyoto 606-8501, Japan (e-mail: yoshi@mech.kyoto-u.ac.jp).

Digital Object Identifier 10.1109/TMECH.2004.823877

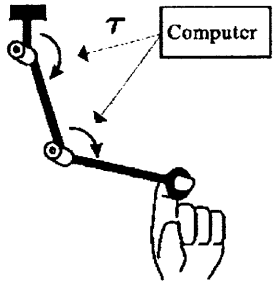

Fig. 1. Conventional haptic device.

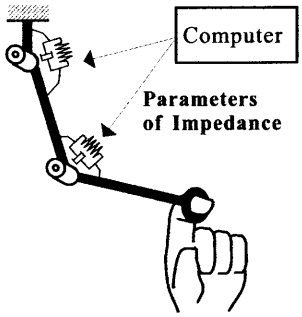

Fig. 2. Proposed haptic device.

The device can generate continuous-time impedance within the sampling period at the fingertip point. Fig. 3 shows an outline of a portion of the analog circuit corresponding to just two joints of the device. In the figure, the mark [+−] represents a differential circuit, the mark [Dif.] represents a differentiation circuit, the mark [Sum.] represents a summing circuit and amplifiers with k_{sp**} and k_{sd**} represent the voltage control amplifier ingegrated circuits (VCA ICs) for the spring element and damping element, respectively; a VCA IC is an amplifier whose gain can be specified using the computer. The potentiometer measures the joint angle. The output from the potentiometer enters the differentiation circuits and the differential amplifier circuits, which subtract the potentiometer output from the command signal u_* of the computer. The output from each circuit is fed back to the motor driver of each joint through a VCA IC. With this circuit, the computer can control the impedance and equilibrium point at the fingertip. The impedance and equilibrium point change discretely at each sampling time, but the force exerted by impedance works continuously even within the sampling period.

C. Dynamics and Kinematics of Device

Kinematics and dynamics of the device including the analog circuit can be expressed as[1]

$$\dot{\boldsymbol{r}} = \boldsymbol{J}\dot{\boldsymbol{q}} \tag{1}$$

$$\boldsymbol{\tau} = \boldsymbol{M}\ddot{\boldsymbol{q}} + \boldsymbol{h} + \boldsymbol{K}_{sp}(\boldsymbol{q} - \boldsymbol{q}_0) + \boldsymbol{K}_{sd}\dot{\boldsymbol{q}} + \boldsymbol{J}^T\boldsymbol{F}_h \tag{2}$$

where $\boldsymbol{r}$ is the fingertip position, $\boldsymbol{q}$ is the joint angle, $\boldsymbol{q}_0$ is the initial position of the potentiometer, $\boldsymbol{F}_h$ is the force exerted by a human operator, $\boldsymbol{M}$ is the inertia matrix, $\boldsymbol{h}$ is the nonlinear matrix containing gravitational, centrifugal and Coriolis forces and $\boldsymbol{J}$ is the Jacobian matrix; $\boldsymbol{K}_{sp}$ and $\boldsymbol{K}_{sd}$ are controllable stiffness and damping coefficients whose elements are given by k_{sp**} and k_{sd**}, respectively

$$\boldsymbol{K}_{sp} = \begin{bmatrix} k_{sp11} & & & k_{sp1n} \\ & k_{spii} \cdots k_{spij} & & \\ & \vdots \quad\quad \vdots & & \\ & k_{spij} \cdots k_{spjj} & & \\ k_{spn1} & & & k_{spnn} \end{bmatrix} \tag{3}$$

$$\boldsymbol{K}_{sd} = \begin{bmatrix} k_{sd11} & & & k_{sd1n} \\ & k_{sdii} \cdots k_{sdij} & & \\ & \vdots \quad\quad \vdots & & \\ & k_{sdij} \cdots k_{sdjj} & & \\ k_{sdn1} & & & k_{sdnn} \end{bmatrix}. \tag{4}$$

Herein, n is the number of joints, $\boldsymbol{\tau}$ is the output force realized by the command signal $\boldsymbol{u} = [u_1 u_2 \cdots u_n]^T$, and the relation between $\boldsymbol{\tau}$ and $\boldsymbol{u}$ is given as

$$\boldsymbol{\tau} = \boldsymbol{K}_{sp}\boldsymbol{u}. \tag{5}$$

When the stiffness coefficient $\boldsymbol{K}_{sp}$ is a nonsingular matrix, force $\boldsymbol{\tau}$ is arbitrarily given by $\boldsymbol{u}$. In the following discussion, it is assumed that $\boldsymbol{K}_{sp}$ is nonsingular.

Researches of a similar controller with tunable gains and equilibriums of springs and dampers have ever been studied [13], but characteristics of the proposed device are that it can also control gains k_{spij} and k_{sdij} which work between joints, and that it is applied to a haptic interface. Above all, such a controller has a great advantage in a haptic display method with coupling impedance including springs and dampers.

III. Haptic Display for Static Virtual Object

This section explains a method for displaying a static virtual object with the haptic device in the previous section and discusses passivity of a 1-DOF system.

A. Control Algorithm

The basic idea is to control strength and direction of impedance on the fingertip point and to move the equilibrium of the impedance to a contact point on the surface of the virtual object. The control algorithm for displaying a static virtual object is described in the following.

[1] When the finger does not touch a virtual object, stiffness and damping matrices are set as

$$\boldsymbol{K}_{sp} = \boldsymbol{0} \quad \boldsymbol{K}_{sd} = \boldsymbol{0} \quad \boldsymbol{\tau} = \boldsymbol{0}. \tag{6}$$

This means that the actuator makes no output and the operator feels only the dynamics of the device.

[2] When the finger touches a virtual object, a contact point $\boldsymbol{r}_d$ and an object coordinate frame Σ_C are defined on the surface of the virtual object as shown in **Fig. 4.**

[1]Generally, the device includes the dynamics of analog circuit. Further, the relation between the joint torque and fingertip force in (2) is valid when the device stands still. In this paper, we assume that their influence is small and can be omitted for human motion.

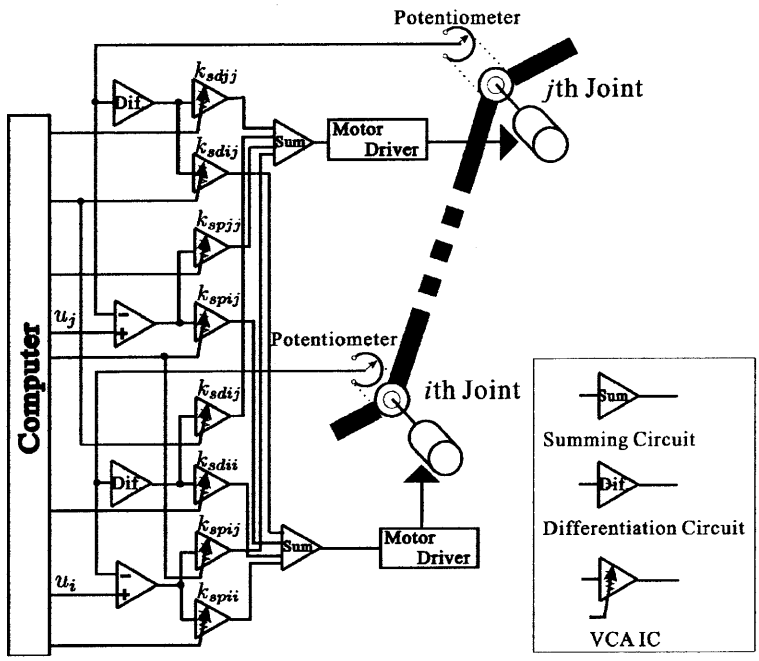

Fig. 3. Outline of analog feedback corresponding to two joints.

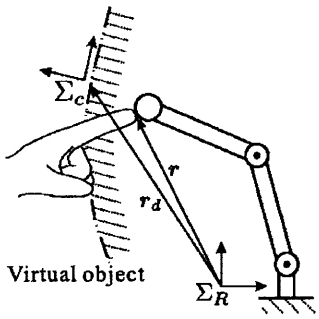

Fig. 4. Object coordinate.

Coupling impedance is defined using stiffness $\boldsymbol{K}_{dp}$ and damping $\boldsymbol{K}_{dd}$ between fingertip position $\boldsymbol{r}$ and contact point $\boldsymbol{r}_d$ along object coordinate Σ_C. Using impedance along Σ_C, stiffness $\boldsymbol{K}_{sp}$ and damping $\boldsymbol{K}_{sd}$ on the circuit are set as

$$\boldsymbol{K}_{sp} = \boldsymbol{J}^T \boldsymbol{R}_c \boldsymbol{K}_{dp} \boldsymbol{R}_c^T \boldsymbol{J} \tag{7}$$

$$\boldsymbol{K}_{sd} = \boldsymbol{J}^T \boldsymbol{R}_c \boldsymbol{K}_{dd} \boldsymbol{R}_c^T \boldsymbol{J} \tag{8}$$

where $\boldsymbol{R}_c$ is the rotational matrix from coordinate Σ_R to coordinate Σ_C.[2] If the actuator output is set as

$$\boldsymbol{\tau} = \boldsymbol{K}_{sp}(\boldsymbol{q}_d - \boldsymbol{q}_0) \tag{9}$$

where $\boldsymbol{q}_d$ is the joint angle for which the fingertip position would be on the contact point $\boldsymbol{r}_d$, then **(2)** becomes

$$\begin{aligned} \boldsymbol{0} &= \boldsymbol{M}\ddot{\boldsymbol{q}} + \boldsymbol{h} + \boldsymbol{K}_{sp}(\boldsymbol{q} - \boldsymbol{q}_d) + \boldsymbol{K}_{sd}\dot{\boldsymbol{q}} + \boldsymbol{J}^T \boldsymbol{F}_h \\ &\simeq \boldsymbol{M}\ddot{\boldsymbol{q}} + \boldsymbol{h} + \boldsymbol{J}^T(\boldsymbol{R}_c \boldsymbol{K}_{dp} \boldsymbol{R}_c^T(\boldsymbol{r} - \boldsymbol{r}_d) \\ &\quad + \boldsymbol{R}_c \boldsymbol{K}_{dd} \boldsymbol{R}_c^T \dot{\boldsymbol{r}} + \boldsymbol{F}_h). \end{aligned} \tag{10}$$

[2]Recently, there are some studies for a renewed relation between fingertip stiffness and joint stiffness when nonzero force is exerted at the fingertip **[14]**. However, a conventional relation for zero- exerted force is considered in this paper.

Note that if $\boldsymbol{r} - \boldsymbol{r}_d$ is small, an approximate expression

$$\boldsymbol{r} - \boldsymbol{r}_d \simeq \boldsymbol{J}(\boldsymbol{q} - \boldsymbol{q}_d) \tag{11}$$

can be used. Equation **(10)** shows that the impedance setting in **(7)** and **(8)** with output **(9)** is equivalent to stiffness $\boldsymbol{K}_{dp}$ and damping $\boldsymbol{K}_{dd}$ along Σ_C.

In addition, higher impedance can be realized by combining software impedance and output **(9)**. In this case, output is given, instead of **(9)**, by

$$\boldsymbol{\tau} = \boldsymbol{K}_{sp}(\boldsymbol{q}_d - \boldsymbol{q}_0) - \boldsymbol{J}^T(\bar{\boldsymbol{K}}_p(\boldsymbol{r} - \boldsymbol{r}_d) + \bar{\boldsymbol{K}}_d \dot{\boldsymbol{r}}) \tag{12}$$

where $\bar{\boldsymbol{K}}_p$ and $\bar{\boldsymbol{K}}_d$ are software stiffness and damping coefficients. The first term of **(12)** is the output to move the equilibrium of impedance realized by the analog circuit; the impedance of this term works continuously within the sampling period. We call this impedance "*continuous-time impedance.*" The second term is impedance exerted directly by the signal $\boldsymbol{u}$ from the computer; the product is a constant force within the sampling period. We call the impedance of this term "*discrete-time impedance,*" which is used conventionally. The impedance on the surface of the virtual object is the sum of the discrete-time impedance and the continuous-time impedance

$$(\bar{\boldsymbol{K}}_p + \boldsymbol{K}_{sp})(\boldsymbol{r}_d - \boldsymbol{r}) + (\bar{\boldsymbol{K}}_d + \boldsymbol{K}_{sd})\dot{\boldsymbol{r}}. \tag{13}$$

This method merely adds a continuous-time impedance to conventional discrete-time impedance. The next section uses passivity analysis to illustrate effects for stability and how the coefficients of the method can be chosen.

B. Passivity Analysis for Displaying a Static Object

1) 1-DOF Display System: To analyze passivity of the method in the previous section, we use a 1-DOF system

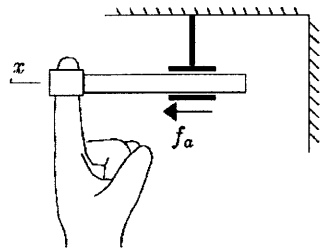

Fig. 5. 1-DOF haptic device.

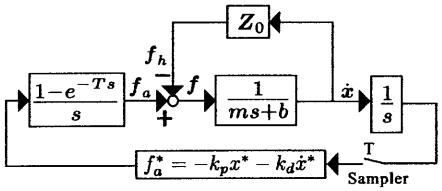

Fig. 6. Block diagram for discrete-time impedance.

as shown in Fig. 5. The dynamic equation of the device is described as

$$f_a = m\ddot{x} + b\dot{x} + f_h \tag{14}$$

where x is the fingertip position, f_a is the exerted force by the actuator, m is the mass of the device, b is the viscosity, and f_h is the force from the operator. We consider a situation when a virtual rigid wall is located at x_d and the operator's finger touches the virtual wall. In that situation, the control algorithm is given as

$$f_a = -k_p(x^* - x_d) - k_d\dot{x}^* \tag{15}$$

where x_* is the sampled data of x, k_p is the stiffness, and k_d is the damping coefficient of the discrete-time impedance.

For such a system, a block diagram is expressed as Fig. 6 and a passivity condition, independent of frequency, was derived by Colgate and Schenkel [3] as

$$b > \frac{k_p T}{2} + k_d \tag{16}$$

where T is the sampling period.

In the case of the proposed method with the electric circuit, the system can be illustrated conceptually as Fig. 7. The dynamic equation is expressed as

$$f_a = m\ddot{x} + b\dot{x} + k_{sp}(x - x_0) + k_{sd}\dot{x} + f_h \tag{17}$$

where k_{sp} and k_{sd} are the coefficients of stiffness and damping by the circuit and x_0 is a position of natural equilibrium. In the haptic display described in the previous section, f_a is given as

$$f_a = k_{sp}(x_d - x_0) - \bar{k}_p(x^* - x_d) - \bar{k}_d\dot{x}^*. \tag{18}$$

The first term is for continuous-time impedance and the second is for discrete-time impedance.

2) Passivity for Displaying a Static Object: A system with continuous-time impedance and discrete-time impedance is expressed by Fig. 8. In the figure, x_d and x_0 are omitted because x_d and x_0 are constant. Since the dynamics of the electric spring

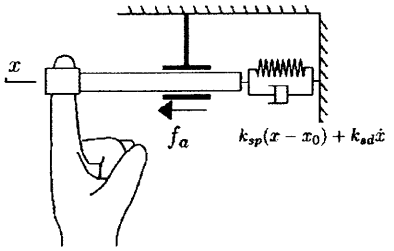

Fig. 7. 1-DOF haptic device with continuous-time impedance.

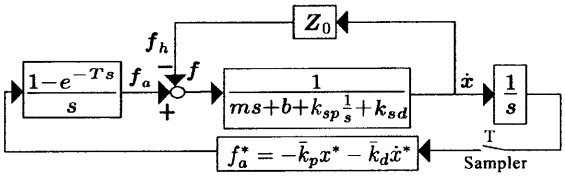

Fig. 8. Block diagram of 1-DOF haptic interface with spring and damper.

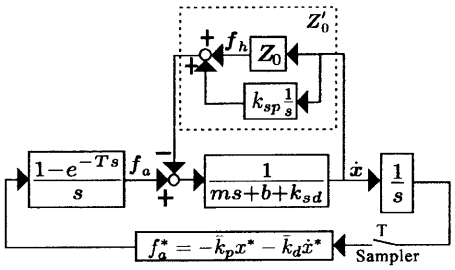

Fig. 9. Modified block diagram of Fig. 8.

can be moved to the operator Z_0, Fig. 8 is equivalent to Fig. 9. In the figure, Z_0' is a system containing the dynamics of the operator Z_0 and the continuous-time spring. If dynamics of operator Z_0 are passive in Fig. 9, that is, if

$$\int_0^{t_f} f_h\dot{x}dt \geq 0 \qquad \forall t_f \geq 0 \tag{19}$$

then, system Z_0' is also passive because

$$\int_0^{t_f} (f_h + k_{sp}x)\dot{x}dt = \int_0^{t_f} f_h dt + \frac{1}{2}[k_{sp}x^2]_0^{t_f} \geq 0. \tag{20}$$

The outer part of system Z_0' is identical to the outer part of system Z in the conventional discrete-time impedance method (Fig. 6) except that b becomes $b + k_{sd}$. This directly implies that a passivity condition is derived as

$$b + k_{sd} > \frac{\bar{k}_p T}{2} + \bar{k}_d. \tag{21}$$

It shows that when continuous-time impedance is used, discrete-time impedance can be set higher according to damping k_{sd} of the continuous-time impedance. Even if $k_{sd} = 0$ in continuous-time impedance, the maximum value of stiffness and damping which are stably displayed to the operator increase to $k_{sp} + \bar{k}_p$ and $k_{sd} + \bar{k}_d$. Further, in the case of the 1-DOF system displaying a static object, there is, theoretically, no upper limit of continuous-time impedance and it is possible to increase continuous-time impedance in the range in which the circuit and amplifier can function practically.

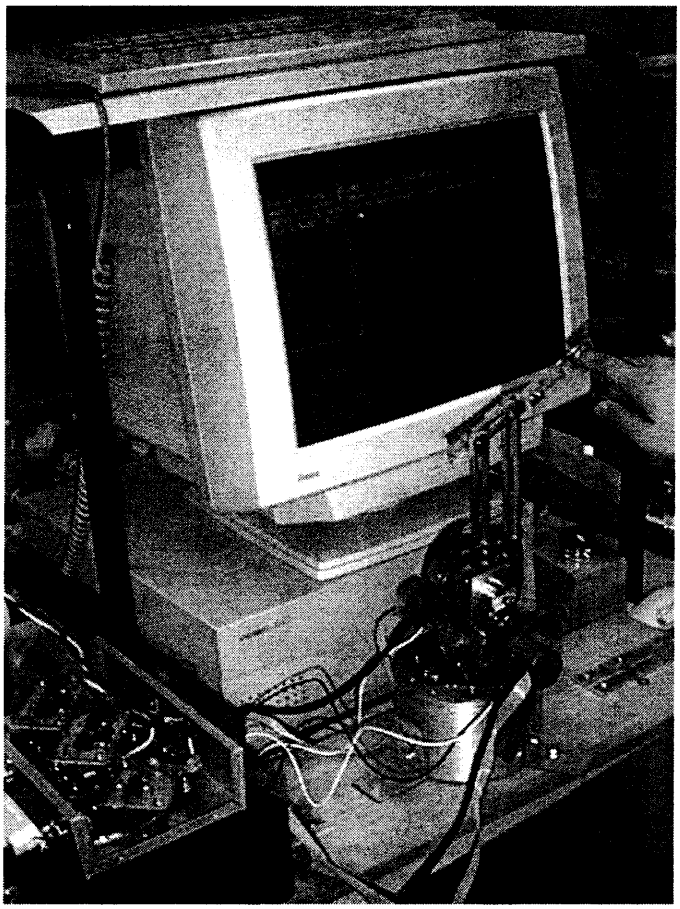

Fig. 10. Overview of experimental setup with 2-DOF haptic display device.

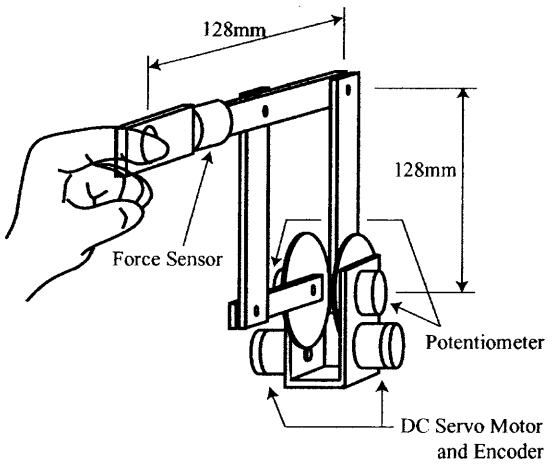

Fig. 11. Specification of 2-DOF haptic display device.

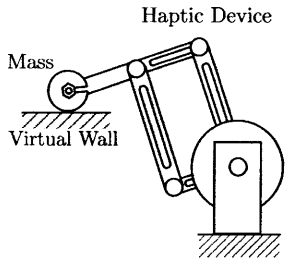

Fig. 12. Experiment for measuring maximum stiffness with a mass.

IV. Experiment

In this section, some experiments with a 2-DOF haptic device and 2-D virtual environment are performed to study the effect of the proposed method.

A. Overview of Experimental Device

Fig. 10 shows an overview of the experimental setup. The haptic device is a 2-DOF robot with linkages whose length is shown in Fig. 11. A dc servomotor actuates a linkage with a gear ratio of 1/8. The rated output of the motor is 11 W and the rated torque is 35 mNm. An encoder, whose resolution is 500 P/R, is installed on the motor; the computer measures angles of each joint with encoders. Potentiometers are used for the proposed analog circuit. The noise of potentiometer is 0.006 rad and the accuracy at the fingertip point is 0.8 mm. A force sensor is installed at the fingertip of the robot and is used only for measuring the experimental result and not for control.

In all experiments, the virtual environment is a simple straight wall with a frictionless surface. Therefore, $\boldsymbol{K}_{dp}$ in (7) and $\boldsymbol{K}_{dd}$ in (8) are

$$\boldsymbol{K}_{dp} = \begin{bmatrix} 0 & 0 \\ 0 & k_{dp} \end{bmatrix} \quad \boldsymbol{K}_{dd} = \begin{bmatrix} 0 & 0 \\ 0 & k_{dd} \end{bmatrix}. \tag{22}$$

B. Experiment for Displaying a Static Object

1) Measuring Maximum Stiffness of Virtual Wall: First, we perform experiments to measure maximum stiffness realizable for a virtual wall by two methods: the discrete-time impedance method and the method of combining continuous-time impedance and discrete-time impedance. Generally, the target of a haptic device is a human, but it is difficult for a human operator to maintain constant conditions and to get objective results. A mass (50 g) is used in the experiment instead of a human. The mass is represented as a point in the virtual environment and is dropped on a virtual floor (Fig. 12). Since the virtual floor has impedance in the virtual environment, the mass bounces on the floor. If the impedance is high, the mass continues to bounce. If it is low, the mass rests on the floor stably. We measure the maximum value of stiffness that makes the mass stop on the floor for each sampling period from 3 to 100 ms. To clarify the comparison, only stiffness is changed and damping is set to zero ($k_d = \bar{k}_d = k_{dd} = 0$). The result is shown in Fig. 13. In the figure, the abscissa is sampling period and the ordinate is stiffness. The dotted line $k_{p\max}$ is the maximum value of the discrete-time stiffness; its relation with the sampling period is inversely proportional, which coincides with (16). The dashed line $\bar{k}_{p\max}$ is the maximum value of the discrete-time stiffness $\bar{k}_p$ when it is used together with the continuous-time stiffness $k_{dp} = 100$ N/m, which is shown by a dashed line in the figure. The value of continuous-time impedance is chosen by trial and error to consider ease of comparison in all ranges of the sampling period from 3 to 100 ms. $\bar{k}_{p\max}$ becomes almost identical to $k_{p\max}$; also, it means that the continuous-time stiffness has no effect on stability of discrete-time stiffness. Note that the stiffness displayed to the real world is the solid line, which is the sum of discrete-time stiffness $\bar{k}_{p\max}$ and continuous-time stiffness k_{dp}.

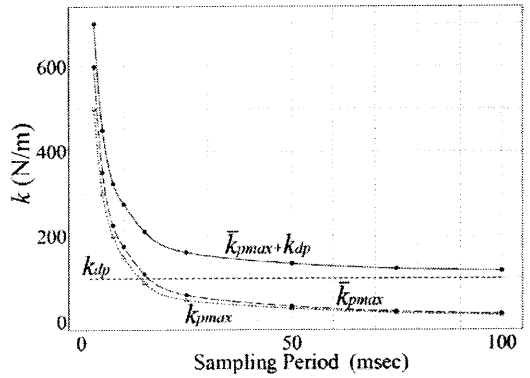

Fig. 13. Result of measuring maximum stiffness with continuous-time spring.

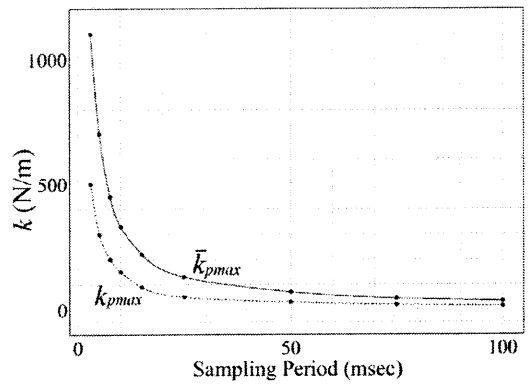

Fig. 14. Result of measuring maximum stiffness with continuous-time damper.

In the experiment, we cannot measure smaller sampling periods than 3 ms and longer sampling periods over 100 ms. For smaller sampling periods, reliable data cannot be measured because an overly large impedance can be set, making it difficult to specify maximum values. For longer sampling periods, impedance is too small and the motion of mass exceeds the motion range of the device.

Fig. 14 shows the result of a case wherein only continuous-time damping k_{dd} is used and continuous-time stiffness k_{dp} is set to zero. In the figure, the solid line $\bar{k}_{p\max}$ is the maximum value of discrete-time stiffness when it is used together with continuous-time damping $\bar{k}_{dd} = 0.002$ Ns/m. In the proposed method, coupling impedance can be increased not only by using continuous-time stiffness, but also by using continuous-time damping.

2) Experiment of Human Operation: Next, we perform some experiments in which the operator traces on a virtual slope with angle $\pi/4$ while trying to apply a constant force for normal direction. In the experiment, the operator can clearly feel a difference between the proposed method and only the discrete-time impedance method. Especially with a long sampling period, the difference can be clearly seen when tracing the virtual slope. On the other hand, the operator feels a rapid change of the reaction force when the finger starts to make contact with the slope because the continuous-time impedance starts to function suddenly at this moment. The feeling of rapid change in the moment is prominent for a long sampling period, when continuous-time impedance is much higher than the maximum value of discrete-time impedance

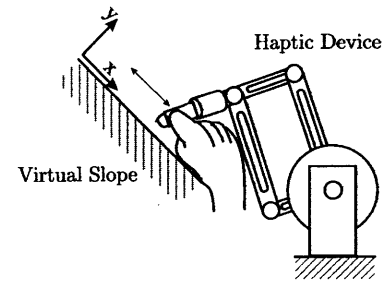

Fig. 15. Experiment for measuring fingertip position and force in human operation.

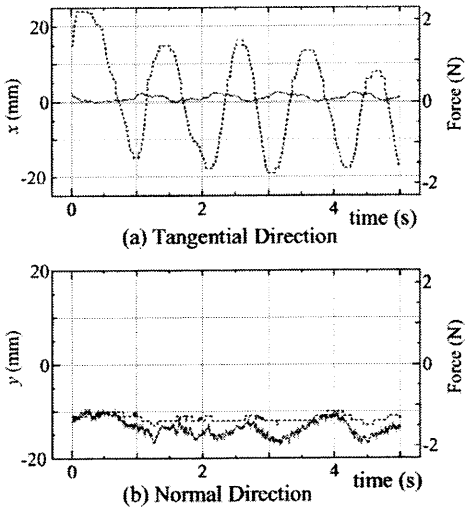

Fig. 16. Result of only discrete-time impedance.

that can be displayed stably. A solution for this behavior will be addressed as a future topic.

As a result of human operation, the fingertip force and position are measured while tracing the slope (Fig. 15). The sampling period is 25 ms. Results of the conventional method with only discrete-time impedance are shown in Fig. 16. In this experiment, discrete-time impedance is chosen as the value which the operator feels to be stable and the stiffness along the normal direction is set to 133 N/m. Fig. 16(a) shows results along the tangential direction of the slope; Fig. 16(b) shows results along the normal direction. In the figures, the solid line indicates the fingertip force and the dotted line shows the fingertip position. Fig. 17 shows results of the proposed method, combining the continuous-time impedance with the discrete-time impedance. The continuous-time stiffness along the normal direction is set to 100 N/m. The sink to the virtual wall, which is the dotted line in Fig. 17(b), is shallower than Fig. 16(b) and it is shown that continuous-time impedance can be stably set higher than the case with only discrete-time impedance.

Finally, we compare the proposed method with a proportional derivative (PD) controller conventionally used. Fig. 18 displays results of a PD controller that is simulated by the proposed device. In this case, stiffness of interference between joints is set to zero and the continuous-time stiffness $\boldsymbol{K}_{sp}$ is a diagonal matrix. It is equivalent to a display using a PD control to the contact point $\boldsymbol{r}_d$ on each joint independently. In the figure, fingertip force along the tangential direction [the solid line in Fig. 18(a)]

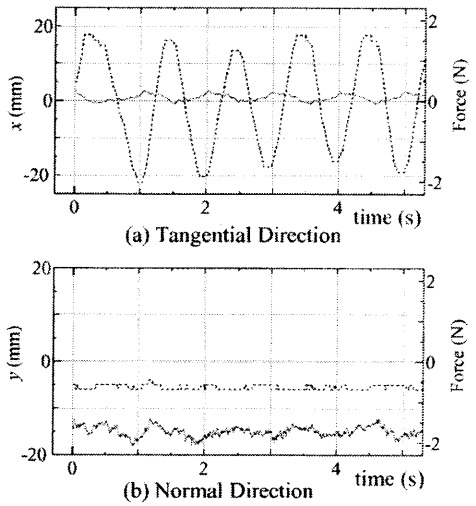

Fig. 17. Result of discrete-time impedance with continuous-time impedance.

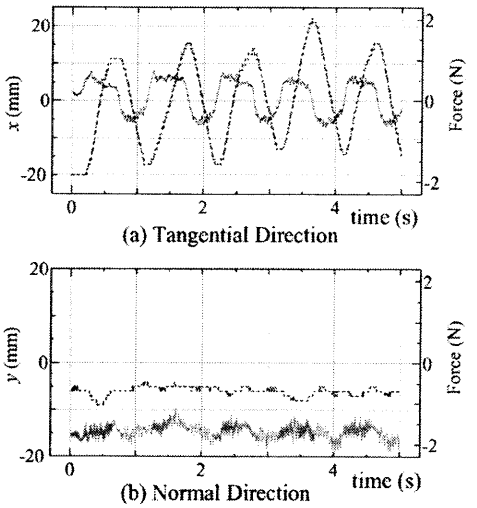

Fig. 18. Result of continuous-time impedance applied independently to each joint.

is larger than the force in Fig. 17(a). This means that the haptic display with the PD controler causes a large resistant force in the tangential direction. On the other hand, the proposed method can decrease such a resistant force.

V. Conclusion

A haptic interface device with an analog circuit which exerts continuous-time impedance within the sampling period has been proposed. The device can decrease the sampling period influence and can display virtual objects and an environment with a harder surface. It has been shown in the case of one-dimensional environment that the proposed method has better stability properties than the conventional method, using passivity analysis. Finally, some experiments in a 2-D environment have been performed and the validity of the proposed method has been confirmed.

References

[1] T. Massie and K. Salisbury, "The PHANTOM haptic interface: A device for probing virtual objects," in *Proc. ASME Winter Annual Meeting*, vol. 55–1, New Orleans, LA., 1994, pp. 295–300.

[2] M. Minsky, M. Ouh-young, O. Steele, F. P. Brooks, and M. Behensky, "Feeling and seeing: Issues in force display," *Comput. Graph*, vol. 24, no. 2, pp. 235–243, 1990.

[3] J. E. Colgate and G. Schenkel, "Passivity of a class of sampled-data systems: Application to haptic interfaces," in *Proc. American Control Conf.*, 1994, pp. 3236–3240.

[4] J. E. Colgate, M. C. Stanley, and J. M. Brown, "Issues in the haptic display of tool use," in *Proc. Int. Conf. Intelligent Robotics and Systems*, 1995, pp. 140–145.

[5] R. J. Adams and B. Hannaford, "Stable haptic interaction with virtual environment," *IEEE Trans. Robot. Automat.*, vol. 15, pp. 465–474, June 1999.

[6] T. Yoshikawa and H. Ueda, "Haptic virtual reality: Display of operating feel of dynamic virtual objects," in *Proc. 7th Symp. Robotic Research,*, 1996, pp. 214–221.

[7] M. Ouh-Young, D. V. Beard, and F. P. Brooks Jr., "Force display performs better than visual display in a simple 6-D docking task," in *Proc. Int. Conf. Robotics and Automation*, 1989, pp. 1462–1466.

[8] J. E. Colgate and J. M. Brown, "Factors affecting the Z-width of a haptic display," in *Proc. Int. Conf. Robotics and Automation*, 1994, pp. 3205–3210.

[9] D. C. Ruspini, K. Kolarov, and O. Khatib, "Haptic interaction in virtual environment," in *Proc. IEEE/RSJ Int. Conf. Intelligent Robotics and Systems*, vol. 1, 1997, pp. 128–133.

[10] ——, "A framework for multi-contact multi-body dynamic simulation and haptic display," in *Proc. IEEE/RSJ Int. Conf. Intelligent Robotics and Systems*, vol. 2, 2000, pp. 1322–1327.

[11] R. Balaniuk and C. Laugier, "Haptic interface in generic virtual reality systems," in *Proc. Int. Conf. Intelligent Robotics and Systems*, 2000, pp. 1310–1315.

[12] T. Yoshikawa, Y. Yokokohji, T. Matsumoto, and X.-Z. Zheng, "Display of feel for the manipulation of dynamic virtual objects," *Trans. ASME J. Dyn. Syst. Meas. Contr.*, vol. 117, no. 4, pp. 554–8, 1995.

[13] C. Abul-Haj and N. Hogan, "An emulator system for developing improved elbow-prosthesis designs," *IEEE Trans. Biomedical Eng.*, vol. BME-34, pp. 724–737, Sept. 1987.

[14] S.-F. Chen and I. Kao, "Conservative congruence transformation for joint and cartesian stiffness matrices of robotic hands and fingers," *Int. J. Robot. Res.*, vol. 19, no. 9, pp. 835–847, 2000.

Masayuki Kawai received the B.S., M.S., and Ph.D. degrees in mechanical engineering from Kyoto University, Kyoto, Japan, in 1992, 1994, and 2000, respectively.

From 1994 to 1997, he was a Mechanical Engineer with Ishikawajima-harima Heavy Industries, Japan, working on factory automation and system design of industrial logistic systems. Since 2000, he has been with Fukui University, Fukui, Japan, where he is currently an Associate Professor in the Center for Cooperative Research in Science and Technology. His current research interests include robotics and haptic virtual reality.

Tsuneo Yoshikawa (M'73–SM'98–F'00) received the Ph.D. degree in applied mathematics and physics from Kyoto University, Kyoto, Japan, in 1969.

Since 1969, he has been with Kyoto University, where he is currently a Professor of Mechanical Engineering. From 1973 to 1975, he was a National Research Council Resident Research Associate at NASA Marshall Space Flight Center, Huntsville, AL. He is the author of *Foundations of Robotics* (Cambridge: MA, MIT Press, 1990). His current research interests include robotics, haptic virtual reality, and mechatronics.

He has received several awards, including the 1995 JDSMC Best Paper Award from the Dynamic Systems and Control Division of the ASME and the 1997 ICRA Best Conference Paper Award from the IEEE Robotics and Automation Society.